2006

Analysis of Scroll Thrust Bearing

Masao Akei
Emerson Climate Technologies/Copeland Corporation

Hong Teng
Emerson Climate Technologies/Copeland Corporation

Kirill M. Ignatiev
Emerson Climate Technologies/Copeland Corporation

ANALYSIS OF SCROLL THRUST BEARING

Masao Akei*, Hong Teng, Kirill M. Ignatiev

Copeland Corporation, Research Department,
Emerson Climate Technologies
1675 West Campbell Road, Sidney, Ohio 45365-0669, U.S.A.
*Phone: 937-498-3167, E-mail: makei@copeland-corp.com

ABSTRACT

Several analytical models on scroll thrust bearings were investigated and compared with the experiment using an actual scroll compressor. With the rigid-body model allowing the orbiting flat plate only to tilt against the thrust bearing, the calculated hydrodynamic oil-film pressure could only carry scroll's axial force acting within the limited range of location on the bearing. On the other hand, the newly-proposed model considering an additional effect of material deformations showed load-carrying characteristics that allowed the axial force locus to be beyond the limitations of the rigid-body wobbling model. The tentative result of the oil-film pressure distribution from the model including deformation showed a better agreement with the experimental results than those from the simpler rigid-body model.

1. INTRODUCTION

Thrust bearings used in scroll compressors have shown excellent load-carrying capability and low-frictional characteristics, which are important contributing factors for those compressors to exhibit superior performance and efficiency. While such attractive bearings have been widely employed in a variety of size of the compressors, technical grounds for their operation have not been satisfactorily clarified yet. Kulkarni (1990) firstly proposed a lubrication model for the scroll thrust bearing. His model adopting a rigid-body dynamics of an orbiting plate predicted the wobbling motion of the orbiting scroll. This phenomenon had been confirmed in actual compressors by experiments (*e.g.*, Hirano et al., 1988). On the other hand, a couple of other analytical studies have been reported recently. Oku et al. (2004) and Sato et al. (2004) analyzed their own lubrication models with assumed surface shapes or tilting angles of the orbiting plate. Although their analytical results were confirmed by experiments using a bench-test apparatus, none of those models have openly been verified in its practical validity on actual compressors.

In the present paper, the above mentioned rigid-body model was firstly re-evaluated to confirm its analytical characteristics on the scroll thrust bearing lubrication. Secondly, the analytical results were compared with the experimental ones obtained from an actual operating compressor in order to verify its practical effectiveness. Finally, based on the findings in the comparison, bearing surface material deformation effect was added to the lubrication model and the combined (complex) model was solved simultaneously. The tentative result from the complex model showed a better agreement with the experiments than that of the rigid-body one.

2. LUBRICATION MODEL WITH SOLID WOBBLING OF ORBITING SCROLL

In order to analyze the characteristics of fluid-film bearings, Reynolds equation, which employs several simplifications of Navier-Stokes Equation and the continuity equation, is widely used. The following Reynolds equation includes the wedge and the squeeze terms for generating the hydrodynamic pressure on a bearing surface. To consider a circular object such as thrust bearing, it can be expressed in cylindrical coordinates r and θ as:

$$\frac{1}{r}\frac{\partial}{\partial r}\left(rh^3\frac{\partial p}{\partial r}\right)+\frac{1}{r^2}\frac{\partial}{\partial \theta}\left(h^3\frac{\partial p}{\partial \theta}\right)=6\eta\left\{\frac{1}{r}\frac{\partial}{\partial r}\left(rhU_r\right)+\frac{1}{r}\frac{\partial}{\partial \theta}\left(hU_\theta\right)+2\frac{\partial h}{\partial t}\right\} \quad (1)$$

Extracting above gives:

$$\frac{\partial^2 p}{\partial r^2}+\left(\frac{3}{h}\frac{\partial h}{\partial r}+\frac{1}{r}\right)\frac{\partial p}{\partial r}+\left(\frac{1}{r^2}\right)\frac{\partial^2 p}{\partial \theta^2}+\left(\frac{1}{r^2}\frac{3}{h}\frac{\partial h}{\partial \theta}\right)\frac{\partial p}{\partial \theta}=\frac{6\eta}{h^3}\left\{U_r\left(\frac{h}{r}+\frac{\partial h}{\partial r}\right)+U_\theta\left(\frac{1}{r}\frac{\partial h}{\partial \theta}\right)+h\left(\frac{\partial U_r}{\partial r}+\frac{1}{r}\frac{\partial U_\theta}{\partial \theta}\right)+2\frac{\partial h}{\partial t}\right\} \quad (2)$$

In the rigid-body model, allowing the solid orbiting plate to tilt against the thrust surface, the oil-film clearance *h* varies along the thrust surface as:

$$h = h_0 - \tan\alpha \cdot \{r\sin(\theta+\beta) - R_{or}\cos(\phi-\beta)\} \quad (3)$$

where h_0 is the representing value of the oil-film clearance at the center of the orbiting plate, α is the tilting angle of the orbiting plate, and β is the directional angle of the tilting. Definitions of these tilting angles are schematically shown in figure 1.

Differentiating equation (3) with respect to *r*, θ, and *t* will provide the *h* derivatives in equation (2):

$$\frac{\partial h}{\partial r} = -\tan\alpha\cdot\sin(\theta+\beta) \quad (4)$$

$$\frac{\partial h}{\partial \theta} = -r\tan\alpha\cdot\cos(\theta+\beta) \quad (5)$$

$$\frac{\partial h}{\partial t} = \dot{h}_0 - r\left\{\frac{\dot{\alpha}}{\cos\alpha}\sin(\theta+\beta)+\dot{\beta}\tan\alpha\cdot\cos(\theta+\beta)\right\} - R_{or}\left\{\frac{\dot{\alpha}}{\cos\alpha}\cos(\theta-\beta)+(\dot{\phi}-\dot{\beta})\tan\alpha\cdot\sin(\phi-\beta)\right\} \quad (6)$$

In equation (2) U_r and U_θ shows the radial and tangential surface velocities of the orbiting scroll, respectively. At an instantaneous crank position the orbital motion of the scroll brings its velocity vector being constant at any location on the thrust surface. This can be expressed with the following:

$$U_r = U\cos(\theta+\phi),\ U_\theta = -U\sin(\theta+\phi) \quad (7)$$
$$\text{where } U = R_{or}\omega_0$$

Therefore, the partial derivatives of U_r and U_θ in equation (2) can be derived as:

$$\frac{\partial U_r}{\partial r} = 0\ ,\ \frac{\partial U_\theta}{\partial \theta} = -U\cos(\theta+\phi) \quad (8)$$

Where the velocity (dot) terms in equation (6) are concerned, only a complete dynamic model of the orbiting scroll can determine their rigorous values. Although such analysis can be performed along with a bearing model, it would make the numerical system more complicated and increase the computation time extremely. In order to perform systemized analyses, a convenient way that reduces the computation load is anxiously desired.

As far as the scroll thrust bearing goes, however, the following reasonable assumptions regarding the squeeze velocity can be proposed. Since the compression load to the orbiting scroll is fairly constant throughout the revolution, it is likely that the

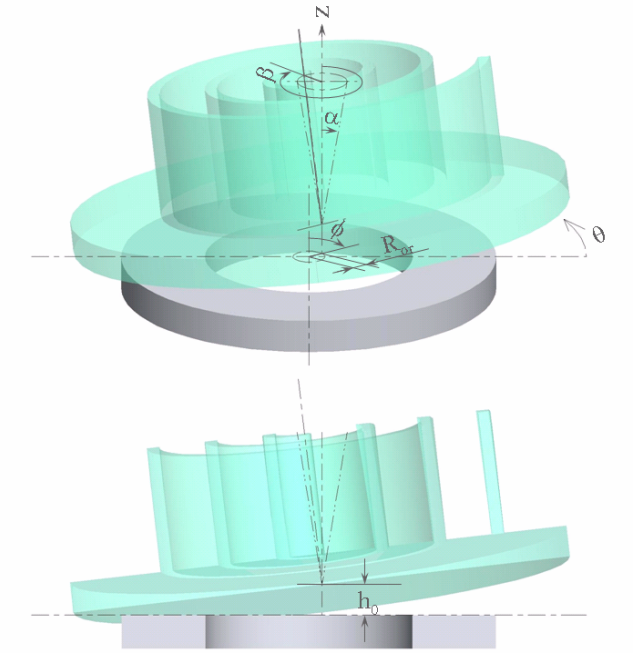

Figure 1: Definitions of coordinates and tilting angles of orbiting scroll.

amount of tilting of the scroll plate as well as its floating distance stays nearly constant [assumption 1]. However, since the orientation of the compression load rotates with the crankangle, the tilted axis (the normal axis of the orbiting plate) should also rotate around the local z-axis with the synchronous speed of crankangle [assumption 2]. Obviously, the local z-axis, which stands on the crank pin, should rotate along the orbiting circle with the crank speed.

With the assumption 1, the following expression can be made:

$$\dot{h}_0 = 0\,, \quad \dot{\alpha} = 0 \tag{9}$$

Also, the assumption 2 and its following sentence can be summarized as:

$$\dot{\beta} = \dot{\phi} = \omega_0 \tag{10}$$

With these assumptions, equation (6) becomes reduced to:

$$\frac{\partial h}{\partial t} = -r\omega_0 \tan\alpha \cdot \cos(\theta + \phi) \tag{11}$$

The equation (11) essentially provides the effect of "even" squeezing (wobbling) as if the h distribution on the thrust surface, which will be defined by h_0, α, and β, rotates with the speed of crankangle. This effect can be expressed in another way by referring equation (5):

$$\frac{\partial h}{\partial t} = \frac{\partial h}{\partial \theta} \cdot \omega_0 \tag{12}$$

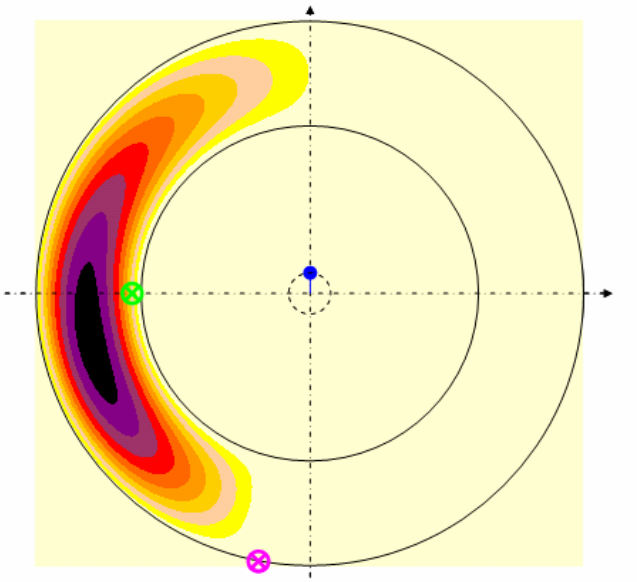

Figure 2: Hydrodynamic oil-film pressure with solid wobbling model of orbiting scroll (The green crossed mark indicates the locus of the oil-film pressure reaction. The pink crossed mark indicates the location of the minimum oil-film thickness. The blue dot shows the location of the crank pin. The crank pin rotates in clockwise.)

A justification of these assumptions can be made by comparing with a complete dynamics. Kulkarni (1990) analyzed the rigid-body dynamics of the orbiting scroll and expected the similar motion of the wobbling on the thrust bearing to the assumed above. In his model h_0, α, and β (i.e.ϕ - β) became not nearly constant since compression load was fluctuating. However, those parameters were quite steady when the lightly fluctuating load that practically occurs at rating condition was applied. Although more detailed investigation is needed for the rigorous justification, it can be claimed at least that the above assumption is useful for the first-order approximation to the squeezing effect.

The integration of equation (2) was carried out with the SOR Method and the restoring force and its locus from the generated hydrodynamic pressure were calculated. The negative pressure that the Reynolds equation generated was ignored and excluded from the integration (Half-Sommerfeld Condition). The iterative Newton-Raphson Method was also used to find the solution of h_0, α, and β, which satisfies balancing in both force and moments between the calculated hydrodynamic pressure and a given input of the axial force and its locus.

Figure 2 shows an example of the calculated pressure distribution of the hydrodynamic-oil film. As for the input of the axial force, its locus was set behind the crank pin against its rotational direction with a certain distance so that its location matches to one of the axial forces from actual scroll compressors (shown with the green crossing mark). For this given input of locus, the tilting orientation of the orbiting plate has been relaxed at 70-80 degree behind from the direction toward the locus of the axial force. The phase difference between the directions towards the locus and the plate-tilting was considered due to the "wobbling" orbiting plate to create the squeezing effect around the location of the targeted locus. With regard to the minimum film thickness, it also appeared in the same direction of the tilting at the outer edge of the thrust bearing due to the assumption of the "rigid" flat plate (shown with the pink crossed mark).

Figure 3 shows how the change in the location of the locus influences on the minimum oil-film thickness of the scroll thrust bearing. As seen in the figure, although the minimum oil-film thickness varied with the force locations in both radial and circumferential directions, it was found that the variation was more significant in the radial direction. As the locus was moved outward, the minimum oil-film thickness became nearly zero and could not keep the appropriate floating distance from the thrust surface. On the other hand, as the force location moved inwards, although the minimum oil-film thickness tended to remain a positive value, any tilting angles could not realize the hydrodynamic pressure having its locus being at such inner location. This was due to the fact that the rigid-body model generates the hydrodynamic pressure being distributed in "U-shape" on the circular thrust surface (*e.g.*, figure 2) and such pressure distribution can only locate its locus at certain distant position from the bearing center. In fact, this tendency became more significant when a larger bearing load was applied, which brought about the U-shape distribution being more concentrated on one side of the bearing, resulting in the locus location being more offset. In the analysis with the rigid-body wobbling model, it is concluded that the thrust bearing can only function in a hydrodynamic mode under the axial force within a limited range of magnitude and locus location zone; axial forces beyond those limitations may cause unwanted bearing behavior like metal to metal contact, wear, or mechanical instability.

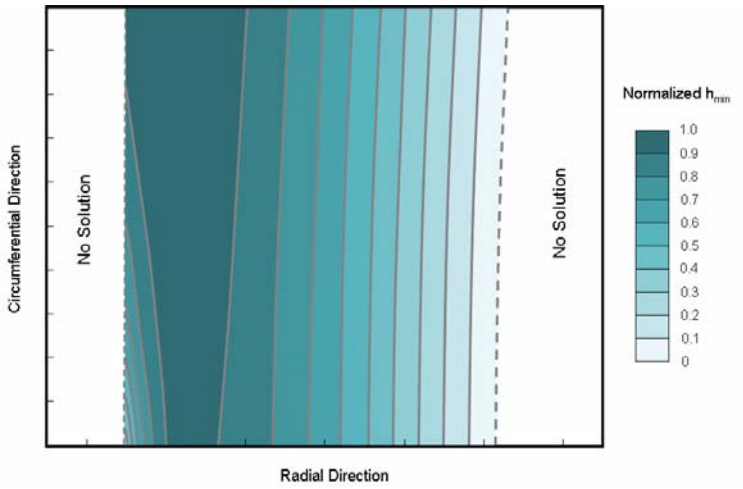

Figure 3: Effect of locus location on minimum oil-film thickness (2-D contour plot)

3. EXPERIMENTAL OBSERVATION OF HYDRODYNAMIC PRESSURE

In actual compressors, however, the thrust bearings perform well while their axial forces act outside of the boundary, limiting the hydrodynamic mode of lubrication predicted by the rigid-body model. This may indicate the presence of other factors also influencing the hydrodynamic film-forming mechanism of the thrust bearing. In order to clarify the discrepancies between the theoretical model and real applications, an experiment was carried out using an actual scroll compressor.

The experiment was designed so that the key parameter of the hydrodynamic pressure on the thrust surface can be compared between the theory and the experiment. The hydrodynamic pressure was measured by mounting pressure transducers on the thrust surface. The transducers were placed so that their diaphragm sections were located almost flush to the thrust surface. Voids in the sensing section of the transducers were filled with a rubber type of resin to minimize the effect of compressible gas being trapped in the voids. The location of the transducers on the thrust surface is shown in figure 4. The obtained pressure transducer signals were numerically interpolated to visualize pressure distribution on the thrust surface.

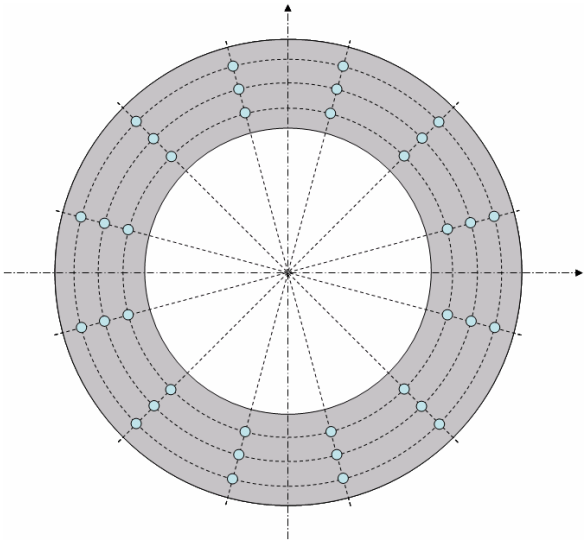

Figure 4: Location of the pressure transducers mounted on the thrust surface (shown with the blue circles)

Figure 5 shows a snap-shot of the pressure distribution on an actual thrust bearing. As seen in the figure, it was found that the hydrodynamic pressure was being formed in "U-shape", which was somewhat similar to the ones predicted by the rigid-body model. However, the experimentally obtained U-shape pressure band was formed mainly at the inner-side of the surface and was further extended in circumferential direction compared to what the rigid-body model predicted. It was also noticed that such extended-pressure band resulted in its locus being located closer to the center of the bearing than the inner radial boundary of the hydrodynamic lubrication zone of the rigid-body model, which allows the thrust bearing to react against the wider range of the axial force than predicted by the latter.

Considering the well-known fact that the base plate of the orbiting scroll is deformed under the loading of the compressed gas, this could lead to a different bearing clearance distribution *h*, which could bring a different oil-pressure distribution on the surface. For further understanding of the scroll thrust bearing, it is concluded that the effect of material deformation needs to be considered in the analysis.

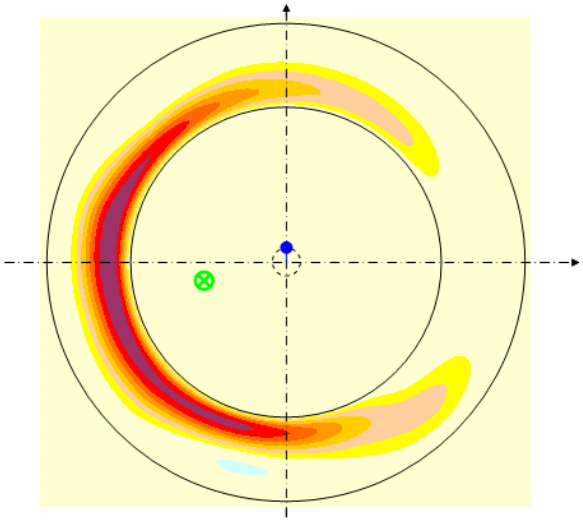

Figure 5: Measured hydrodynamic oil-film pressure in a scroll compressor and its locus.

4. LUBRICATION MODEL WITH MATERIAL DEFORMATION

In order to consider the effect of deformations, FEA models consisting of the orbiting scroll as well as the thrust bearing were employed and combined with the Reynolds equation. Since the *h* distribution in the Equation (2) will be affected by the deformation, equation (3) needs to be modified slightly as:

$$h = h_0 - \tan\alpha \cdot \{r\sin(\theta+\beta) - R_{or}\cos(\phi-\beta)\} + \delta \qquad (13)$$

where δ is the total deformation of the orbiting plate and the thrust bearing on its surface. The *h* derivatives in terms of *r* and θ can be approximated with the central difference formula:

$$\frac{\partial h}{\partial r} = \frac{h_{r+\Delta r} - h_{r-\Delta r}}{2\Delta r}, \frac{\partial h}{\partial \theta} = \frac{h_{\theta+\Delta\theta} - h_{\theta-\Delta\theta}}{2\Delta\theta} \qquad (14)$$

Regarding the squeeze term in the Reynolds equation, the same assumption of wobbling motion as developed in the rigid body model was adopted. By referring the equation (12):

$$\frac{\partial h}{\partial t} = \frac{\partial h}{\partial \theta}\cdot\omega_0 = \frac{h_{\theta+\Delta\theta} - h_{\theta-\Delta\theta}}{2\Delta\theta}\cdot\omega_0 \qquad (15)$$

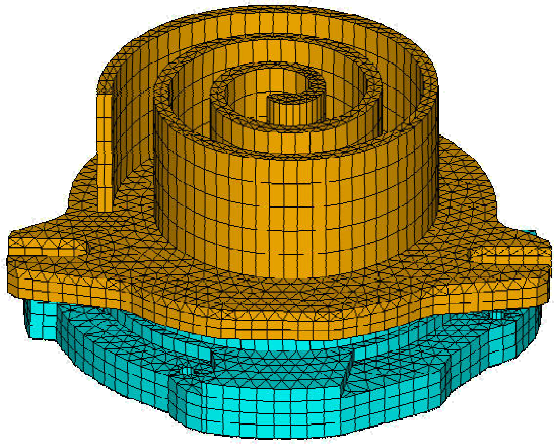

Figure 6: FEA model used in the calculation to consider the effect of deformation on hydrodynamic film-forming characteristics.

The calculation was made in two steps. First, initial h_0, α, and β were given to the program and calculated the corresponding δ that balances with the hydrodynamic oil-film pressure on the thrust surface. Second, above calculation was iterated until the respective δ were converged. Gas compression load and its corresponding force were directly applied to the orbiting scroll as it occurs in an actual compressor. Figure 6 shows the schematic of the FEA model used in the calculation.

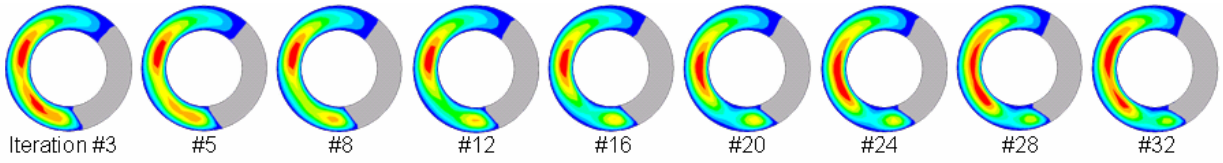

Figure 7: Interim outputs of the oil-film pressure distribution during the iterative process of the calculation (The numbers indicate the sequence of iteration).

Figure 7 shows the sequence of the interim outputs during the iteration of the calculation. Unfortunately, since the above squeeze term in the Reynolds equation induces a significant influence on hydrodynamic pressure, the numerical system of the model has become quite stiff and challenging to solve. As it can be seen in the figure, the calculated outputs oscillate around the possible solution, and having not yet obtained the full convergence. In order to see the significance of this squeeze effect on the hydrodynamic film-forming characteristics, we have also tried to exclude the squeeze effect from the Reynolds equation. In this trial, the model became quite steady and the convergence have been achieved (Figure 8). This difference in the numerical system should be indicating that the squeeze effect in the Reynolds equation plays a significant role in the oil-film pressure generation.

Figure 9 is the enlarged picture from the oscillating outputs, which showed the smallest difference in oil-film pressure distribution between the iteration steps (Iteration #24). By comparing the case with the squeeze effect excluded with one where it is included, it was found that both models showed their oil-film pressure distributions being biased toward the inner radius of the thrust bearing. This was due to the fact that, regardless of the existence of the squeeze effect, both the orbiting scroll and the thrust bearing were deformed by the interaction between the given compression force and the oil-film pressure, resulting in creating the smaller oil-film thickness at the inner radius of the thrust bearing (Figure 10). In both cases, the calculated oil-pressure distributions were closer to the experiments than those of the rigid-body model. It can be concluded that the effect of deformation should also play a certain role in creating such a hydrodynamic pressure distribution, which balances the axial force with the locus being beyond the limitation of the hydrodynamic locus location, which was predicted by the rigid-body motion model.

Further studies are currently in progress in finalizing the calculation to the squeeze effect. Further assessments will be remarked at the time of presentation.

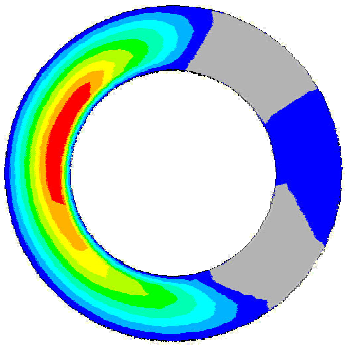

Figure 8: Calculated hydrodynamic oil-film pressure with the deformation model (Excluding the squeeze effect).

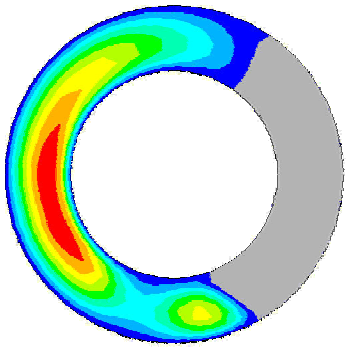

Figure 9: Calculated hydrodynamic oil-film pressure with the deformation model (Interim results including squeeze effect).

Figure 10: Oil-film thickness distribution on the thrust surface (The darker the blue the smaller the oil-film thickness).

5. CONCLUSIONS

The hydrodynamic film-forming characteristics of a thrust bearing used in scroll compressors were investigated with several analytical models and experiments. Following remarks have been concluded from this study:

- Hydrodynamic lubrication model of the thrust bearing, which considers only the rigid-body motion of the flat orbiting scroll, limits the possible location of the axial force locus in order for the hydrodynamic oil-film lubrication to exist.
- The experimentally observed thrust bearing hydrodynamic oil-film pressure distribution was to a certain degree different from the one obtained from the solid body motion model. The experimentally obtained oil-film pressure was mainly formed at the inner side of the thrust bearing and its high pressure band was significantly extended in circumferential direction compared to the rigid body motion model results.
- Hydrodynamic lubrication model, which considers both rigid body motion and deformation of the scroll and thrust bearing, but excludes the squeeze effect from the Reynolds equation, shows oil-film pressure distribution closer to those of the experimentally obtained one; also, it proves the existence of hydrodynamic oil-film lubrication beyond the locus location limitations of the rigid body motion model.
- Hydrodynamic lubrication model, which considers rigid-body motion and deformation of the scroll and thrust bearing, as well as both wedge and squeeze effect from the Reynolds equation, shows that squeeze effect plays a significant, if not a dominant role in the oil film pressure generation. However, at the time of preparation of the present paper, only preliminary results of the latter model were available to the authors.
- Further studies aimed at assessing the effect of oil film squeeze effect are currently under way.

NOMENCLATURE

h	oil-film thickness	(m)
h_0	oil-film thickness at crank pin	(m)
p	oil-film pressure	(Pa)
R_{or}	orbiting radius	(m)
U_r	radial surface velocity	(m/s)
U_θ	tangential surface velocity	(m/s)
α	tilting angle	(rad)
β	directional angle of tilting	(rad)
δ	total deformation on bearing surface	(m)
ϕ	crank angle	(rad)
η	viscosity	(Pa s)
ω_0	crank angular speed	(rad/s)

Subscripts

r	radial coordinate
θ	angular coordinate

REFERENCES

Hirano, T., Matsumura, N., Takeda, K., 1988, Development of High Efficiency Scroll Compressors for Air Conditioners, *International Compressor Engineering Conference at Purdue*: p. 65-74.

Kulkarni, S. S., 1990, Thrust Bearing Design under Laminar Conditions, *International Compressor Engineering Conference at Purdue*: p. 327-332.

Kulkarni, S. S., 1990, Thrust Bearing Design with Rigid Body Dynamics of the Runner Plate, *International Compressor Engineering Conference at Purdue*: p. 333-344.

Oku, T., Anami, K., Ishii N., Sano, K., 2004, Lubrication Mechanism at Thrust Slide-bearing of Scroll Compressors (Theoretical Study), *International Compressor Engineering Conference at Purdue*: C104.

Sato, H., Ito, T., Kobayashi H., 2004, Frictional Characteristics of Thrust Bearing in Scroll Compressor, *International Compressor Engineering Conference at Purdue*: C027.

ACKNOWLEDGEMENT

The authors would like to express their appreciation to Jim Fogt, Sunil Kulkarni and Jean-Luc Caillat for their fruitful discussions on this study.